RSC Advances

ROYAL SOCIETY OF CHEMISTRY

www.rsc.org/advances

ARTICLE

Indole-based pH Probe with Ratiometric Fluorescence Behavior for Intracellular Imaging

Received 00th January 20xx,
Accepted 00th January 20xx

DOI: 10.1039/x0xx00000x

www.rsc.org/

Ming Nan,[a] Weifen Niu [a] ,Li Fan[a], Wenjing Lu[a], Shaomin Shuang[a], Chenzhong Li[b], Chuan Dong[a*]

3-[3-(4-Fluorophenyl)-1-(1-methylethyl)-1H-indol-2-yl]-(E)-2-propenal(FMIP) was used as a ratiometric fluorescent pH probe with favorable optical properties for strong-acidity pH detection in living cells. The probe exhibits ratiometric fluorescence emission ($I_{528\ nm}/I_{478\ nm}$) characteristics with pK_a 3.90 and linear response to strong-acidity range of 3.3–4.5. The major features of the probe include large Stokes shift (163 nm at pH 7.0 and 113 nm at pH 3.5), high selectivity and good photostability. More importantly, the probe has excellent cell membrane permeability and is further applied successfully to monitor pH in living cells.

1.Introduction

Intracellular pH plays the vital roles in various cellular behaviors and pathological processes, such as receptor-mediated signal transduction, enzymatic activity[1], endocytosis[2], cell proliferation, apoptosis[3, 4], ion transport and homeostasis[5], drug resistance[6]. Disruption of normal cytoplasmic and organellar pH homeostasis or even slight changes would have a great impact on the progress of distinct pathophysiologic states and even cause cancer[7, 8], cardiopulmonary and neurologic problems such as Alzheimer's disease[9, 10]. As a consequence, sensing intracellular pH values and monitoring their fluctuation would provide indispensable information for the further understanding of the physiological and pathological processes closely relevant to pH.

Fluorimetry has attracted considerable attention over many other methods due to its high sensitivity, noninvasiveness, and fast response time. Moreover, with the combination of fluorescent probes and confocal laser scanning microscopy, fluorescent imaging provides high spatial and temporal observation of pH changes in live cells[11]. Currently, numerous excellent pH-dependent fluorescent probes with near neutral (pH6-8)[12-17] or weak acidic (pH4-6)[18-21] response behavior have been exploited for applications in biological systems. Unfortunately, very few research was involved at pH below 4. Despite the fact that most of the living species could hardly live in highly acidic conditions (pH < 4), there still exists a considerable number of microorganisms, such as helicobacter pylori and "acidophiles", that particularly favor this harsh living conditions[22, 23] . Another example is enteric pathogens, which may possibly lead to fatal infections by means of passing through the strongly acidic mammalian stomach and reaching the small intestine. Moreover, in some eukaryotic cells, acidic pH plays a critical role in numerous organelles along the secretory and endocytic pathways. [24, 25] . Because of lacking effective ways to detect such acidic pH in living species, the precise pH values in these cellular compartments remain elusive. Thus, monitoring the very low intracellular pH conditions is still a challengable issue.

Chen and co-workers[26] first developed a protein-based pH probe HdeA58-DMN for noninvasive measurement of the extremely acidic pH in *E. coli*cells. The probe with the genetically encoded nature made the intracellular pH detection in diverse prokaryotic and eukaryotic species come true. Subsequently, Zhao *et al.* [27]reported a fluorescent probe based on coumarin and imidazole derivative for detection of extreme acidity (pK_a = 2.1) in bacteria. More recently, they designed some other pyrazoline-based pH fluorescent probes which were used for imaging strong acidity in *Saccharomyces cerevisiae* [28]. However, the current fluorescent probes are mainly focused on single emission intensity measurement. It is to some extent difficult to avoid the influence of instrumental efficiency, probe concentration and optical path length because of the single emission band[11, 29]. Whereas, ratiometric fluorescent probes allow the measurement of changes in the intensity ratio of two emission bands induced by analyte and offer the more reliable analysis. Therefore, the ratiometric fluorescent probes exhibit excellent advantages over single emission intensity measurement in living cells. Bojinov *et al.* [30] reported a ratiometric pH probe based on rhodamine–naphthalimide with a pK_a value of 3.7 and detectable pH range of the probe was from 2 to 5. Zhao *et al.* [31]recently developed a ratiometric probe with coumarin–rhodamine FRET system and utilized it for measurement of extreme acidity in *E. coli*

[a] *Institute of Environmental Science, School of Chemistry and Chemical Engineering, Shanxi University, Taiyuan 030006, People's Republic of China.*
[b] *Nanobiosensors/Bioelectronics Laboratory, Department of Biomedical Engineering, Florida International University, Miami, FL 33174, USA*
E-mail: dc@sxu.edu.cn; Fax: +86-351-7018613; Tel: +86-351-7018613

cells. Our previous research fabricated a pH fluorescent probe with ratiometric fluorescence emission characteristics and applied it to monitor pH fluctuations in live cells and imaging extreme acidity in *Escherichia coli* cells[32]. These reports encouraged our efforts towards exploring novel ratiometric pH probes with facile preparation, large Stokes shift, high sensitivity and good photostability for low acidity measurement.

3-[3-(4-Fluorophenyl)-1-(1-methylethyl)-1H-indol-2-yl]-(E)-2-propenal (FMIP) (Scheme 1) was commonly used as an important drug precursor for synthesizing fluvastatin and their analogues[33], antibacterial agents and antifungal agents[34] and anti-inflammatory medicine[35]. For structure concern, FMIP contains electron-accepting substituents (-F) and electron-donating substituents (the nitrogen atom in indole) with the D– π –A structure that may be available to possess intramolecular charge transfer (ICT) fluorescent properties and the nitrogen atom of indole moiety is sensitive to protonation and deprotonation. Moreover, the protonation would significantly change the electron-donating properties of the nitrogen atom of the indole unit with the result that the hybrid indole-based acrolein derivative would generate a ratiometric response to pH in the acidic window. Above thinking induces us to extend the optical behavior and utility of FMIP. Interestingly, we found fluorescence of FAMP with ratiometric emission characteristics and exhibited pH dependence especially in the case of strong acidity. Moreover, it is expanded to intracellular imaging under strong acidity with satisfying results.

2.Materials and methods

2.1 Chemicals and instruments

3-[3-(4-Fluorophenyl)-1-(1-methylethyl)-1H-indol-2-yl]-(E)-2-propenal (FMIP) was commercially available. Deionized water was used throughout all experiments. All solvents were purchased from commercial suppliers in analytical grade and used without further purification. The solutions of metal ions were prepared from nitrate salts or chloride salts which were dissolved in deionized water. Dilute hydrochloric acid was used for tuning pH values.

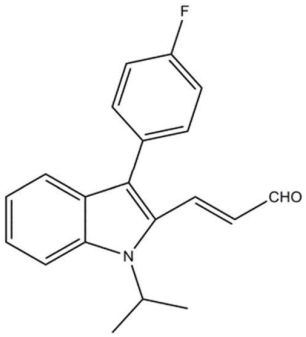

FMIP

Scheme 1 Molecular structure of FMIP

Absorption spectra were recorded on a TU-1901 double-beam UV–vis spectrophotometer (Beijing Purkinje General Instrument Co., Ltc., Beijing, China). Fluorescence measurements were carried out on a Varian Cary Eclipse fluorescence spectrophotometer with excitation and emission slits setting at 5.0 nm and 10.0 nm respectively. Fluorescence images of BIU-87 cells were obtained using FV1000 confocal laser scanning microscope (Olympus Co.,Ltd. Japan) with an objective lens (×40). pH values were measured with a Beckman Φ50 pH meter (Shanghai LeiCi Device Works, Shanghai, China). Deionized water was obtained from a Milli-Q water purification system (Millipore).

2.2 UV–Vis and Fluorescence pH Titrations

Absorption spectra were recorded in 1 cm × 1 cm quartz cuvettes on TU-1901 UV–vis spectrophotometer. Fluorescent emission spectra were collected from 400 nm to 700 nm on Varian Cary Eclipse fluorescence spectrophotometer with excitation wavelength of 365 nm, the excitation and emission slit widths were 5 nm and 10 nm, respectively. Probe FMIP was dissolved in ethanol for a stock solution(1mM). The solutions for absorption and fluorescence spectroscopic determination were obtained by diluting the stock solution to 25 μM in water medium. In the pH titration experiments, 3 mL solution of FMIP was poured into a quartz optical cell of 1 cm optical path length, and the solutions were modulated for different pH by adding the minimum volumes of HCl. Spectral data were recorded after each addition. Unless otherwise specified, the experiments were performed at room temperature (20±3°C) for the convinence purpose.

2.3 Cytotoxicity assays

According to the literature[16], the MTT (3-(4,5 dimethylthiazol -2-yl)-2,5- diphenyltetrazolium bromide) assay was used to test the cytotoxicity of FMIP to HeLa cells. The cells with a density of 1×10^5 cells per mL were cultured in a 96-well microplate to a total volume of 100 μL per well at 37 ℃ in a 5% CO_2 atmosphere. After 24 h, different concentrations of FMIP of 0.5 μM, 1 μM, 10 μM, 15 μM and 20 μM were incubated with HeLa cells for 4 h in fresh medium, respectively. Cells in a culture medium without FMIP were used as the control. After washing the cells with cold phosphate buffered saline (PBS, pH 7.4) three times, 10 μL of MTT solution (10 mg•mL^{-1}, PBS) was added into each well of the 96-well microplate for another 4 h. Then, the remaining MTT solution was removed from the wells and 150 μL of DMSO was added into each well to dissolve the intracellular blue-violet formazan crystals. The absorbance value of the solution was measured at 490 nm wavelength. The cell viability was calculated by the following equation:

$$\% \text{ viability} = [\Sigma(A_i/A_{control} \times 100)]/n$$

where A_i is the absorbance of different concentrations of

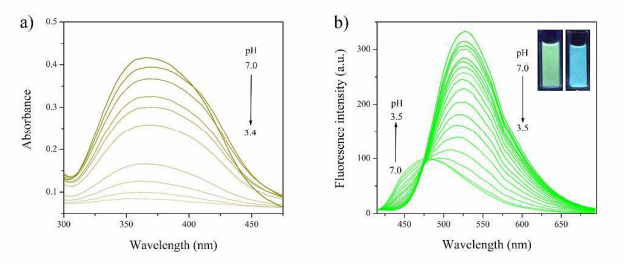

Figure 1. (a) Change of absorption spectra of FMIP as pH decreased from 7 to 3.4. (b) Change of fluorescence spectra of FMIP as pH decreased from 7 to 3.5 (λ ex = 365 nm). The inset shows photographs of the probe at pH=7 and pH=3.5 under UV light (λ ex=365 nm).

the probe of 0.5 μM, 1 μM, 10 μM, 15 μM and 20 μM, respectively. Acontrol is the average absorbance of the control well in which the probe was absent, and n (=5) is the number of the data point.

2.4 Cell culture and confocal imaging

BIU-87 were cultured in Dulbecco's modified Eagle's medium (DMEM) supplemented with 10% fetal bovineserum (FBS), and the cells were seeded in the culture dish and cultured at 37 °C in a 5% CO_2 atmosphere for 48 h. Then the culture medium was removed, and the cells were washed with phosphate-buffered saline (PBS). FMIP dissolved in DMSO was added into PBS buffers at various pH and incubated with cells for an additional 30 min at 37 °C. The concentration of FMIP in the buffer solutions was controlled at 10 μM. After that, the cells were washed three times in PBS buffers at various pH to remove excess FMIP. Fluorescence images were collected on a confocal laser scanning microscope.

3.Results and discussion

3.1 Absorption and emission properties of the probe

To study the optical responses of FMIP to pH, standard pH titrations of absorption spectra and fluorescence emission spectra were performed. Figure 1a shows the UV-vis absorption spectral change of FMIP under the conditions of varying pH. The probe displays an obvious absorption band at 365 nm (ε=9.95×103 M^{-1} cm^{-1}, at 365 nm, pH = 7). With the decrease in pH values from 7 to 3.5, the absorption peak at around 365 nm of the probe significantly diminished.

The pH titration indicates that the probe exhibits remarkable pH-dependent behavior in emission spectra (Figure 1b). Green fluorescence (λ_{em}= 528 nm) is strong at neutral and weak acidic conditions but gradually quenches with the increase of acidity under 365 nm excitation. Simultaneously, a new blue-shift emission appears at 478 nm with an obvious hypsochromic shift of 50 nm and a distinct isoemission point at 478 nm. One explanation would be that the proton quickly reacted with the nitrogen atom in the indole unit under acidic conditions (as shown in Scheme 2). This would lead to a decrease in the electron-donating ability of the nitrogen atom to participate in the π -electron conjugation at the final stage. Thus a significant blue shift in emission spectra is observed, which indicates equilibrium between the deprotonated and protonated forms of the hybrid indole-based acrolein derivative (Scheme 2). Further proof of the equilibrium is obtained by the observation of notable color changes from green to blue under ultraviolet light (inset of Figure 1b), when the pH decreases.

Since fluorescence bands with maxima at 478 and 528 nm are significantly overlapped, the ratio of intensities at the wavelengths of corresponding maxima would lead to non-negligible error. Herein, the ratio of $I_{528\ nm}$ with $I_{478\ nm}$ was obtained by deconvoluting the spectrum at every pH into two separate bands peaked at 478 nm and 528 nm and acquiring the ratio of band areas. It is worth noting that the ratiometric calibration of green florescence compared to blue fluorescence is 3.48 at pH 7 and 0.68 at pH 3.5 (Figure 2a). Moreover, nonlinear fit of the sigmoidal curve (emission intensity ratios versus pH value) affords the probe a pK_a value of 3.90. The emission ratio also shows good linearity with pH in the range 3.3-4.5, according to the linear regression equation $I_{528\ nm}/I_{478\ nm}$ = -5.65 + 1.95pH, with a linear coefficient of 0.99 (inset of Figure 2a). Thus, this probe could be potentially suitable for monitoring pH variations in the acidic environments in bio-samples.

Scheme 2. Acid−Base Form Equilibrium

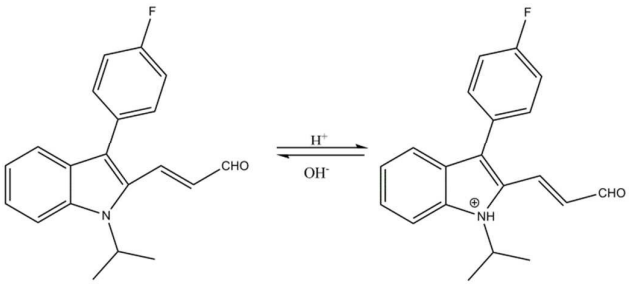

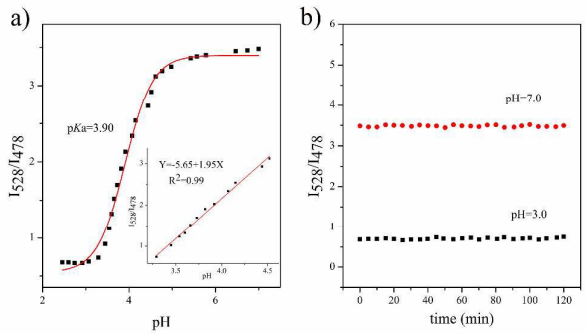

Figure 2. (a) Sigmoidal fitting of ratiometric fluorescence intensity (I_{528}/I_{478}) to various pH values (from 7 to 2.5). (Inset) Linear relationship between I_{528}/I_{478} and pH values in the range pH 3.3-4.5. （b） Changes in fluorescence intensity for FMIP with times at different pH , λ ex = 365 nm.

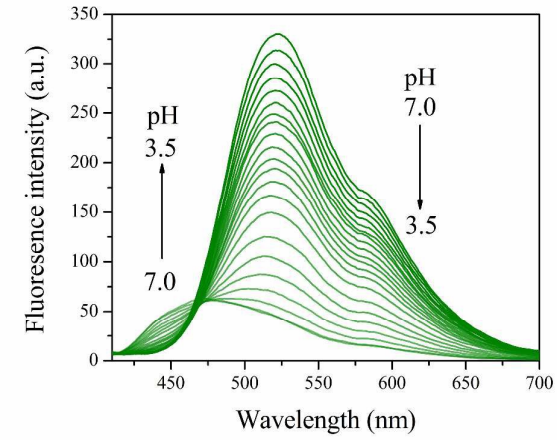

Figure 3. Change of fluorescence spectra of FMIP in the cell medium with pH decreased from 7 to 3.5 (λ ex= 365 nm).

Considering the application of FMIP in the living cells, fluorescence pH titrations were carried out in the presence of cell medium (DMEM) (Figure 3). The properties of the probe in the presence of cell medium are consistent with Figure 1b. It demonstrates that the complex environment of the cell medium should not affect the probe response.

3.2 Photostability

The stability of the probe is tested by measuring the fluorescent response during 2 h. Figure 2b shows the time course of fluorescence intensity of the probe at pH 7.0 and 3.0 at room temperature. The fluorescence intensity is continuously monitored and recorded. The experimental results indicate that the probe can instantly respond to the change of H^+ concentration and the probe solution possesses good photostability. Thus, the probe can be used to monitor pH variation in real time.

3.3 Theoretical calculation

To better understand the optical responses of probe FMIP upon binding with H^+, time-dependent density functional theory (TDDFT) calculations for FMIP with the B3LYP exchange functional employing 6-31+G(d，p) basis sets using a suite of Gaussian 09 programs were conducted. Figure 5 shows the optimized structure and the lowest unoccupied and the highest occupied molecular orbital (LUMO and HOMO) plots of the probe and its protonated form.

It is worth noting that the natural bond orbital charge distributions show N (-0.605*e*) with the most negative charge relative to O (-0.407*e*) and F (-0.296*e*), and that the N atom should be protonated. As shown in Figure 4b, for both FMIP and FMIP－H^+, the S_0 - S_1 (HOMO - LUMO) transitions are electron density redistributions from the indole moiety including the nitrogen atom to the fluorophenyl moiety. Thus, some degree of ICT occurrs in both FMIP and FMIP－H^+. However, upon H^+ binding with the nitrogen atom of the indole unit, in comparison with the electron density distribution in the HOMO and LUMO of FMIP, no electron density in the HOMO and LUMO of FMIP－H^+ is located on the nitrogen atom, demonstrating that the electron-donating ability of the nitrogen atom is weakened, which is unfavorable for the ICT effect. In addition, TDDFT calculations indicate that the HOMO–LUMO energy gap of FMIP－H^+ (3.59 eV) is significantly higher than that of probe FMIP (3.35 eV) (Figure 4b), which is in good agreement with the observation that FMIP exhibits a blue shift lower pH values (Figure 1b).

3.4 Selectivity experiment of different metal ions

The selectivity of FMIP to H^+ over representative metal ions was also investigated at pH 7.0 and 3.5 by competition experiments, respectively. As shown in Figure 5, physiologically ubiquitous metal ions such as K^+, Na^+, Ca^{2+} and Mg^{2+} over their physiological concentrations do not give any obvious emission change on pH measurement. Other heavy or transition-metal ions, such as Mg^{2+}, Zn^{2+}, Al^{3+}, Ba^{2+}, Ni^{2+}, Cu^{2+}, Co^{2+}, Cd^{2+}, Pb^{2+}, Cr^{3+}, Fe^{3+} were also investigated, no noticeable change is observed in the fluorescence intensity ratio of probes FMIP in neutral and acidic conditions. These results reveal that the probe FMIP shows an excellent selectivity response to pH in the presence of background metal ions.

3.5 Cell Cytotoxicity Assay

Since FMIP shows excellent selectivity to H^+ and high photostability, it is possible to explore its use in intracellular pH imaging. Before that, it is crucial to evaluate the cytotoxicity of FMIP to living cells by MTT assay. Figure 6 depicts the viability of HeLa cells under various probe concentrations from 0.5 μM to 20 μM. The results demonstrate that more than 82% of cells are viable and the maximum concentration tested in MTT assays is larger than that used in subsequent bioimaging study, showing the low

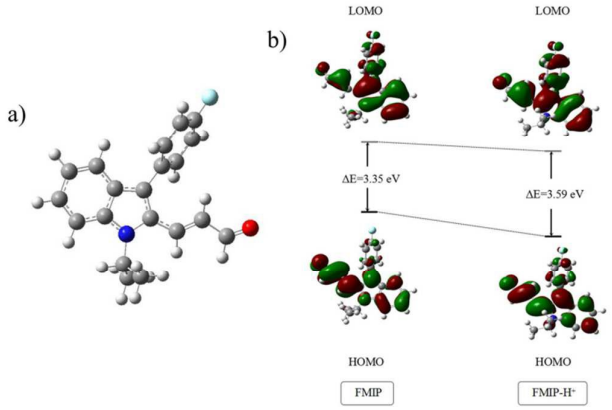

Fig. 4 (a) The optimized structure of probe FMIP determined by DFT calculations. (b) Calculated HOMO and LUMO distributions of FMIP and its protonated form.

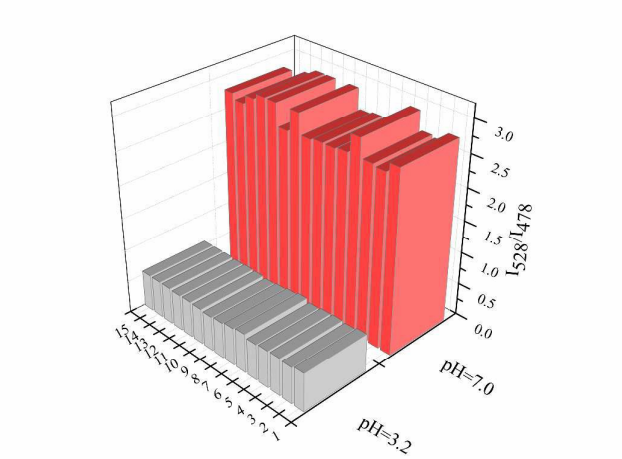

Figure 5. Fluorescence intensity of 25 μM FMIP at different pH in the presence of various species: pH=7, (1) blank; (2) 100 mM Na^+; (3) 133 mM K^+; (4) 10 mM Ca^{2+}; (5) 3.3 mM Mg^{2+}; (6) 77.33 mM Zn^{2+}; (7) 43.3 mM Al^{3+}; (8) 33 mM Ba^{2+}; (9) 16.67 mM Ni^{2+}; (10) 13.3 mM Cu^{2+}; (11) 3.3 mM Co^{2+}; (12) 2 mM Cd^{2+}; (13) 0.5 mM Pb^{2+}; (14) 0.7 mM Cr^{3+}; (15) 0.2 mM Fe^{3+}; pH=3.2, (1) blank; (2) 66.67 mM Na^+; (3) 133.3 mM K^+; (4) 16.67 mM Ca^{2+}; (5) 10 mM Mg^{2+}; (6) 100 mM Zn^{2+}; (7) 60 mM Al^{3+}; (8) 46.67 mM Ba^{2+}; (9) 23.3 mM Ni^{2+}; (10) 53.3 mM Cu^{2+}; (11) 3.3 mM Co^{2+}; (12) 4.5 mM Cd^{2+}; (13) 0.4 mM Pb^{2+}; (14) 0.73 mM Cr^{3+}; (15) 0.3 mM Fe^{3+}. λex = 365 nm.

toxicity of the probe to cultured cells under experimental conditions and inferring their potential use in intracellular imaging of living cells.

3.6 Imaging of Living Cells

In order to explore potential applications in imaging of living cells, the pH-dependent emission changes in living cells were tested. *BIU-87* cells were incubated with probe FMIP (10 uM) for 30 min at 37°C and then the cells were washed in PBS

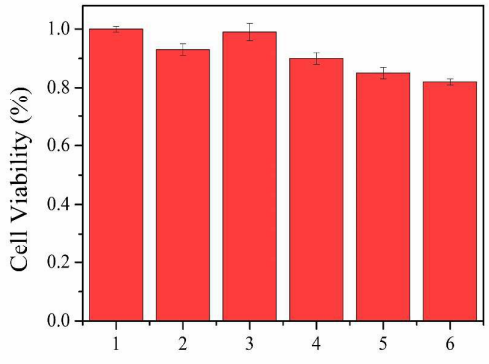

Figure 6. Cell cytotoxic effect of FMIP on HeLa cells. 1, control; 2, 0.5 μM; 3, 1μM; 4, 10 μM; 5, 15μM; 6, 20 μM. Data are expressed as mean values standard error of the mean of five independent experiment.

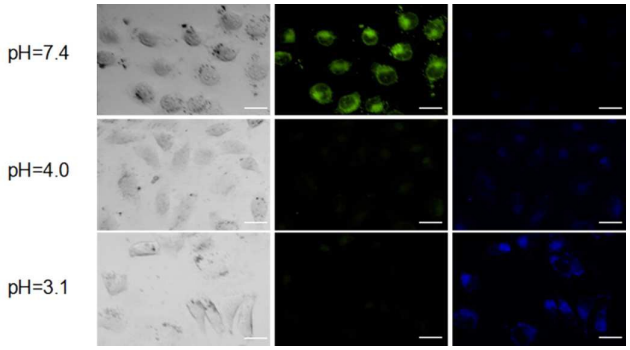

Figure 7. The first column were bright field image of BIU-87 cells incubated with probe FMIP at pH 7.4, 4.0 and 3.1, respectively. The images of the second and third column were collected in green channel (500−550 nm) and blue channel (450−500 nm) with the excitation wavelength 405 nm, respectively. Scale bar: 20 μm.

buffer of varying pH values. The concentration of FMIP in the medium was controlled at 10μM. Fluorescence images are collected on a confocal laser scanning microscope. As shown in Figure 7, it is obvious that the *BIU-87* cells display bright green fluorescence (Figure 7b) and almost no blue fluorescence (Figure 7c) is observed at pH 7.4. However, when the living cells are incubated with the probe FMIP at pH 4.0, a partial quenching in green fluorescence (Figure 7e) and very weak blue fluorescence (Figure 7f) is noted. With the decrease of pH to 3.1, the green fluorescence is almost too low to be observed (Figure 7h); by contrast, the blue fluorescence intensity increases significantly (Figure 7i). These results are consistent with the spectral data shown in Figure 1b. Taken together, these imaging results demonstrated that probe FMIP is cell membrane permeable and could be employed for ratiometric imaging of pH fluctuations in the living cells.

4.Conclusion

In summary, FMIP displays ratiometric response to pH and can detect pH changes in strong acid conditions. The pH titration indicates that as the pH decreases from 7.0 to 3.5, the emission ratio ($I_{578\ nm}/I_{478\ nm}$) also changes dramatically from 3.48 to 0.68. Interestingly, the probe with a pK_a of 3.90 responded linearly and rapidly to minor pH fluctuations within the range of 3.3-4.5. It is also highly significant that FMIP displays a large Stokes shift (163 nm at pH 7.0 and 113 nm at pH 3.5), which can reduce the excitation interference. Furthermore, other advantageous properties of the probe include fine photostability, excellent selectivity and low cytotoxicity, all of which were favorable for intracellular pH imaging. Application of FMIP to pH imaging in live *BIU-87* cells was also achieved successfully, indicating that the probe had good cell membrane permeability and could be used to visualize intracellular pH fluctuations with negligible autofluorescence. It is anticipate for FMIP and its derivatives

would be potential application for cell imaging in the biomedical and biological fields. FMIP represents rationmetric emission property for the extreme acidity detection purpose, making it an effective pH-imaging agent for diverse prokaryotic and eukaryotic species[36, 37]. The development of extreme acidic pH probe would also promote biology study on special biological systems[38].

Acknowledgments

This work was supported by the National Natural Science Foundation of China (No. 21475080 and 21575084), Shanxi Province Hundred Talents Project and Shanxi Scholarship Council of China (No.2013 - key 1).

Notes and references

1 H. A. Clark, R. Kopelman, R. Tjalkens and M. A. Philbert, *Analytical Chemistry*, 1999, **71**, 4837-4843.
2 M. Lakadamyali, M. J. Rust, H. P. Babcock and X. Zhuang, *Proceedings of the National Academy of Sciences of the United States of America*, 2003, **100**, 9280-9285.
3 D. Pérez-Sala, D. Collado-Escobar and F. Mollinedo, *Journal of Biological Chemistry*, 1995, **270**, 6235-6242.
4 R. A. Gottlieb, J. Nordberg, E. Skowronski and B. M. Babior, *Proceedings of the National Academy of Sciences*, 1996, **93**, 654-658.
5 P. Donoso, M. Beltrán and C. Hidalgo, *Biochemistry*, 1996, **35**, 13419-13425.
6 S. Simon, D. RoY and M. Schindler, *Proceedings of the National Academy of Sciences*, 1994, **91**, 1128-1132.
7 M. Schindler, S. Grabski, E. Hoff and S. M. Simon, *Biochemistry*, 1996, **35**, 2811-2817.
8 H. Izumi, T. Torigoe, H. Ishiguchi, H. Uramoto, Y. Yoshida, M. Tanabe, T. Ise, T. Murakami, T. Yoshida, M. Nomoto and K. Kohno, *Cancer Treatment Reviews*, 2003, **29**, 541-549.
9 H. S. Mogensen, D. M. Beatty, S. J. Morris and O. S. Jorgensen, *Neuroreport*, 1998, **9**, 1553-1558.
10 T. Davies, R. Fine, R. Johnson, C. Levesque, W. Rathbun, K. Seetoo, S. Smith, G. Strohmeier, L. Volicer and L. Delva, *Biochemical and biophysical research communications*, 1993, **194**, 537-543.
11 J. Han and K. Burgess, *Chemical reviews*, 2009, **110**, 2709-2728.
12 B. Tang, F. Yu, P. Li, L. Tong, X. Duan, T. Xie and X. Wang, *Journal of the American Chemical Society*, 2009, **131**, 3016-3023.
13 J. Han, A. Loudet, R. Barhoumi, R. C. Burghardt and K. Burgess, *Journal of the American Chemical Society*, 2009, **131**, 1642-1643.
14 E. Nakata, Y. Yukimachi, Y. Nazumi, Y. Uto, H. Maezawa, T. Hashimoto, Y. Okamoto and H. Hori, *Chemical communications*, 2010, **46**, 3526-3528.
15 U. C. Saha, K. Dhara, B. Chattopadhyay, S. K. Mandal, S. Mondal, S. Sen, M. Mukherjee, S. van Smaalen and P. Chattopadhyay, *Organic Letters*, 2011, **13**, 4510-4513.
16 L. Fan, Q. Liu, D. Lu, H. Shi, Y. Yang, Y. Li, C. Dong and S. Shuang, *Journal of Materials Chemistry B*, 2013, **1**, 4281.
17 J. Zhou, C. Fang, T. Chang, X. Liu and D. Shangguan, *J. Mater. Chem. B*, 2013, **1**, 661-667.
18 X. Du, N. Y. Lei, P. Hu, Z. Lei, D. H. Ong, X. Ge, Z. Zhang and M. H. Lam, *Analytica chimica acta*, 2013, **787**, 193-202.
19 H. S. Lv, S. Y. Huang, B. X. Zhao and J. Y. Miao, *Analytica chimica acta*, 2013, **788**, 177-182.
20 H. S. Lv, S. Y. Huang, Y. Xu, X. Dai, J. Y. Miao and B. X. Zhao, *Bioorganic & medicinal chemistry letters*, 2014, **24**, 535-538.
21 H.-S. Lv, J. Liu, J. Zhao, B.-X. Zhao and J.-Y. Miao, *Sensors and Actuators B: Chemical*, 2013, **177**, 956-963.
22 H. Li, H. Guan, X. Duan, J. Hu, G. Wang and Q. Wang, *Organic & biomolecular chemistry*, 2013, **11**, 1805-1809.
23 M. Tian, X. Peng, J. Fan, J. Wang and S. Sun, *Dyes and Pigments*, 2012, **95**, 112-115.
24 T. A. Krulwich, G. Sachs and E. Padan, *Nat Rev Micro*, 2011, **9**, 330-343.
25 G. Loving and B. Imperiali, *J Am Chem Soc*, 2008, **130**, 13630-13638.
26 M. Yang, Y. Song, M. Zhang, S. Lin, Z. Hao, Y. Liang, D. Zhang and P. R. Chen, *Angewandte Chemie International Edition*, 2012, **51**, 7674-7679.
27 Y. Xu, Z. Jiang, Y. Xiao, F. Z. Bi, J. Y. Miao and B. X. Zhao, *Analytica chimica acta*, 2014, **820**, 146-151.
28 X. Zhang, S.-Y. Jing, S.-Y. Huang, X.-W. Zhou, J.-M. Bai and B.-X. Zhao, *Sensors and Actuators B: Chemical*, 2015, **206**, 663-670.
29 Z. Xu, K.-H. Baek, H. N. Kim, J. Cui, X. Qian, D. R. Spring, I. Shin and J. Yoon, *Journal of the American Chemical Society*, 2009, **132**, 601-610.
30 K. A. Alamry, N. I. Georgiev, S. A. El-Daly, L. A. Taib and V. B. Bojinov, *Journal of Luminescence*, 2015, **158**, 50-59.
31 S.-L. Shen, X.-F. Zhang, S.-Y. Bai, J.-Y. Miao and B.-X. Zhao, *RSC Adv.*, 2015, **5**, 13341-13346.
32 W. Niu, L. Fan, M. Nan, Z. Li, D. Lu, M. S. Wong, S. Shuang and C. Dong, *Anal Chem*, 2015, **87**, 2788-2793.
33 J. T. Zacharia, T. Tanaka and M. Hayashi, *The Journal of organic chemistry*, 2010, **75**, 7514-7518.
34 K. V. Gaikwad, S. D. Rathod, S. B. Sawant, D. V. Kale, S. B. Jadhav and S. V. Gaikwad, *Org. Chem.: Indian J.*, 2009, **5**, 167-172.
35 S. D. Rathod, K. V. Gaikwad, S. V. Gaikwad and S. B. Jadhav, *Org. Chem.: Indian J.*, 2008, **4**, 451-457.
36 L. Fan, S.-Q. Gao, Z.-B. Li, W.-F. Niu, W.-J. Zhang, S.-M. Shuang and C. Dong, Sensors and Actuators B: Chemical, 2015, 221, 1069-1076.
37 J. Chao, Y. Liu, J. Sun, L. Fan, Y. Zhang, H. Tong and Z. Li, Sensors and Actuators B: Chemical, 2015, 221, 427-433.
38 M. Su, Y. Liu, H. Ma, Q. Ma, Z. Wang, J. Yang and M. Wang, Chemical communications, 2001, 960-961.

